Regeneration of Airy pulses in fiber-optic links with dispersion management of the two leading dispersion terms of opposite signs

R. Driben and T. Meier

Department of Physics and CeOPP, University of Paderborn, Warburger Strasse 100, D-33098 Paderborn, Germany

(Received 4 February 2014; published 14 April 2014)

Dispersion management of periodically alternating fiber sections with opposite signs of two leading dispersion terms is applied for the regeneration of self-accelerating truncated Airy pulses. It is demonstrated that for such a dispersion management scheme, the direction of the acceleration of the pulse is reversed twice within each period. In this scheme the system features light hot spots in the center of each fiber section, where the energy of the light pulse is tightly focused in a short temporal slot. Comprehensive numerical studies demonstrate a long-lasting propagation also under the influence of a strong fiber Kerr nonlinearity.

DOI: 10.1103/PhysRevA.89.043817 PACS number(s): 42.25.Bs, 42.65.−k, 42.81.Dp

I. INTRODUCTION

In recent years the interest in fascinating self-accelerating Airy light waves has increased significantly due to their unusual fundamental properties and their application potential [1–6]. While other types of waves such as nonlinear solitary waves may experience an acceleration (central frequency shift) as a result of interaction with other waves [7], the acceleration of Airy light waves is an inherent property. The Airy beams have a multipeak shape and propagate along bending trajectories. Airy pulses [8–14], the counterparts of spatial Airy beams, propagate with their acceleration resulting from a varying group velocity. Studies of multidimensional spatiotemporal Airy light bullets have also been presented [12,15]. Applications of Airy waves include plasmonic routing [16], particle cleaning [17], and supercontinuum generation [11]. Recently, the observation of an electron Airy beam has also been reported [18].

The dynamics of truncated Airy pulses launched into a fiber close to its zero-dispersion point under the action of second- and third-order dispersion (TOD) has been investigated [19–21]. It was demonstrated that the joint action of the TOD and the second-order dispersion (SOD) with the same sign leads to variations in the curvature of the trajectory [19]. On the other hand, when the pulse dynamics is governed by TOD with a sign opposite to that of the second-order dispersion (SOD) term, the Airy pulse reaches the tight-focusing point, then undergoes an inversion, and, finally, continues to propagate with an opposite acceleration [20]. At the focal point, the pulse is concentrated in a very narrow and intense light spot (hot spot). Under the action of SOD and TOD with comparable strengths, the focal point extends into a finite area, from which the pulse reemerges with its acceleration reversed [20]. Interestingly, reversing the acceleration of Airy waves in the spatial domain was recently demonstrated by applying a nonlinear three-wave mixing process in an asymmetrically poled nonlinear photonic crystal [22].

It was found that the linear propagation of the truncated Airy wave, which is suitable for a practical realization, in a fiber with SOD leads to a final diversion of the wave [8]. Very recently, a scheme based on dispersion management (DM) [23] was proposed for the increase of Airy pulse longevity [24]. TOD with the same sign as SOD was also taken into account. In general, any initial field distribution can be recovered using the DM method, and limitations start to rise only in the nonlinear regime.

Here, we analyze and compare the possibilities to regenerate truncated Airy pulses by applying a DM scheme that consists of alternating fiber sections with opposite signs of the second-order dispersion term that is similar to the one in [24], with the regeneration possibilities in another scheme having alternation of the two leading dispersion terms. In the scheme with the alternation of both the second and the third dispersion terms it will be demonstrated that the acceleration of the Airy pulse will experience multiple reversals which are accompanied by the creation of multiple hot spots in the course of the propagation in the dispersion-managed fiber link. The latter scheme will reveal a long-lasting propagation with multiple tight light concentration hot spots in the course of the propagation. This regime of tight pulse compression persists in the presence of strong fiber Kerr nonlinearity and provides the possibility to describe the system performance in a quantitative way as a function of the injected light peak power.

II. THE MODEL

The evolution of truncated Airy pulses in lossless fiber links with alternating signs of SOD and TOD of opposite signs is considered. The evolution is governed by the normalized nonlinear Schrödinger equation:

$$i\phi_\xi + (-1)^n(1/2)\phi_{TT} + (-1)^{n+1}(i/6)\varepsilon\phi_{TTT} + |\phi|^2\phi = 0. \tag{1}$$

An odd-integer index n represents sections with negative SOD and positive TOD, while an even-integer index n stands for fiber sections with positive SOD and negative TOD. The normalized distance is given by: $\xi = z|\beta_2|/T_0^2$ and the relative TOD strength by the parameter $\varepsilon = \beta_3/\beta_2/T_0$ where β_2 and β_3 are the second- and third-order dispersion parameters of the fiber sections, and T_0 is the pulse width. The Kerr nonlinearity is represented by the last term.

In general the SOD parameter can be very small if one operates near the zero-dispersion point of a fiber. In the case of a very steep slope of the dispersion the relative TOD-SOD parameter ε can take large values. Strictly speaking, a generalized nonlinear Schrödinger equation [25] including the Raman and shock terms would describe the model more precisely in such cases. Still, the Raman term may be excluded in fibers such as hollow-core photonic-crystal fibers filled with Raman inactive gas [26], and the shock term does not change the system behavior in a significant manner as direct numerical simulations including this term have demonstrated.

III. DYNAMICS IN THE QUASILINEAR REGIME

In the case of the negligible TOD parameter (for example, for pulses with a long duration) the third term in Eq. (1) can be dropped, and a classical DM scheme with compensation of only the SOD applies. An example of the application of the dense DM scheme [27] to the Airy pulse is presented in Fig. 1(a) for five representative scheme periods with fibers connections of $\xi = 4$. We can see that the pulse shape is

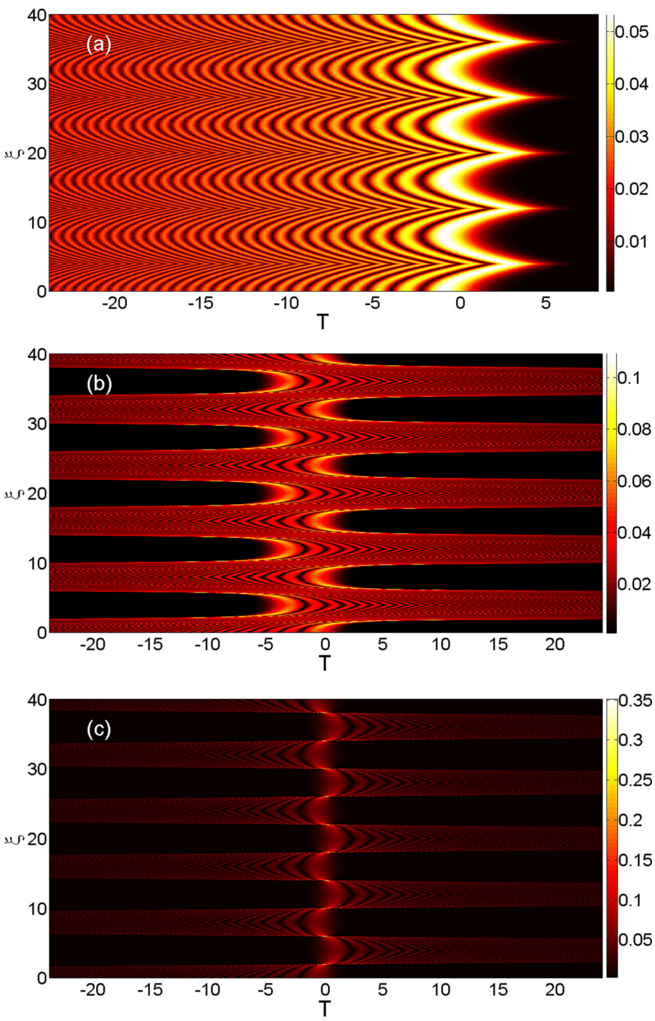

FIG. 1. (Color online) (a) The dynamics of the Airy pulse in the quasilinear regime in a DM scheme with alternation of only SOD ($\epsilon = 0$). (b) The dynamics of Airy pulses in five periods of the DM scheme under the action of equal-strength SOD and TOD, with $\epsilon = -1$ in Eq. (1). (c) The dynamics under the action of strongly dominant TOD with $\epsilon = -1000$. Here and below, all results are presented in normalized units. Here and Fig. 2 the absolute value of the field is shown instead of the intensity for better visibility of the low-power regions of the pulse.

periodically recovered during the propagation. For shorter pulses, usually, the role of TOD increases, and we have to take into account its influence on the dynamics of Airy pulses [19–21,24]. In practice, if we make fiber connections too frequent, losses associated with these connections will play a stronger role. On the other hand, if we connect the compensating section too far from the preceding one, the pulse will exceed its initial temporal slot. We chose an optimal regime for the system performance to preserve the original pulse width working with each fiber section's length:

$$L = 2/\varepsilon, \tag{2}$$

and thus one period of the DM scheme is $2L$. Practically, an Airy pulse can be produced by adding a cubic phase to the spectrum of a simple Gaussian, i.e., the input for Eq. (1) will be $\varphi_0(\omega) = \exp(-\alpha\omega^2 + i\omega^3/3)$, with $\alpha > 0$. In the low-power propagation regime, the nonlinear term in Eq. (1) can be dropped, and the input in frequency representation can be substituted into Eq. (3), which is a transformed version of Eq. (1):

$$\psi_\xi = (i/2)\mathrm{sgn}(\beta_2)\omega^2\psi + (1/6)\varepsilon\omega^3\psi. \tag{3}$$

After the inverse Fourier transform the analytic solution for the pulse evolution in odd and even fiber links reads

$$|\varphi(\xi',T)|^2 = 2\pi\theta^{2/3}|\mathrm{Ai}[\theta^{1/3}(T - 0.25\theta\xi'^2 + \alpha^2\theta + i\alpha\theta\xi')]|^2 \times \exp\left(2\alpha\theta T + \tfrac{4}{3}\alpha^3\theta^2 - \theta^2\alpha\xi'^2\right) \tag{4}$$

for odd fiber sections with $\xi' = \xi - 2nL$ and

$$|\varphi(\xi'',T)|^2 = 2\pi\theta^{2/3}|\mathrm{Ai}[-\theta^{1/3}(T - 0.25\theta\xi''^2 + \alpha^2\theta - i\alpha\theta\xi'')]|^2 \times \exp\left(-2\alpha\theta T - \tfrac{4}{3}\alpha^3\theta^2 + \theta^2\alpha\xi''^2\right) \tag{5}$$

for compensating even fiber sections with $\xi'' = \xi - (2n + 1)L$. The parameter θ is given by $\theta = 1/(0.5\varepsilon\xi + 1)$. In the center of each of the fiber sections with $0.5\varepsilon\xi = 1$, the pulse reaches its most compressed state, and the pulse profile is Gaussian and is given by [20]

$$|\varphi(T)|^2 = \frac{1}{2\sqrt{\alpha^2 + 1/\varepsilon^2}} \exp\left(-\frac{T^2}{2\alpha + 2/(\alpha\varepsilon^2)}\right). \tag{6}$$

The given analytic solutions were compared to the results of direct numerical simulations of Eq. (1), and complete agreement was found. The pulses are launched as [8]

$$\varphi_0 = A\mathrm{Ai}(T)\exp(\alpha T), \tag{7}$$

with the truncation parameter $\alpha > 0$. Figure 1(b) demonstrates the evolution of low-power Airy pulses with amplitude $A = 0.1$ for the case of joint action of SOD and TOD of equal strengths. In this regime, near the middle of each section of the link the Airy pulse reaches a finite area of recombination and afterwards experiences an acceleration reversal. The size of the area depends on the relative strength of the SOD and TOD coefficients.

Next, we consider the dynamics of the low-peak-power Airy pulses under the dominant action of TOD over SOD, which is relevant when pulses are launched very close to the zero-dispersion point of the fiber [Fig. 1(c)]. In the regime of TOD domination the recombination area converges into a very short temporal slot, featuring hot spots with tight focusing in the time domain with all of the pulse's energy concentrated in it. As we can see, the DM scheme provides a successful restoration of Airy pulses in the low-power regime that, in practice, is only limited by the fiber's attenuation.

IV. DYNAMICS IN THE STRONGLY NONLINEAR REGIME

Launching pulses in the high-power strongly nonlinear regime leads to some deterioration of the system performance, although the main effects remain qualitatively valid. Figures 2(a) and 2(b) demonstrate distortion with the propagated distance of the Airy pulse launched in a fiber link as in Fig. 1, but with an amplitude $A = 3$ [30 times higher than in the case of Figs. 1(a) and 1(b)]. Figure 2(a) demonstrates the distorted dynamics in the nonlinear regime using the regular DM scheme with compensation of only SOD, while Fig. 2(b) demonstrates the same pulse evolution in a scheme with management of both SOD and TOD.

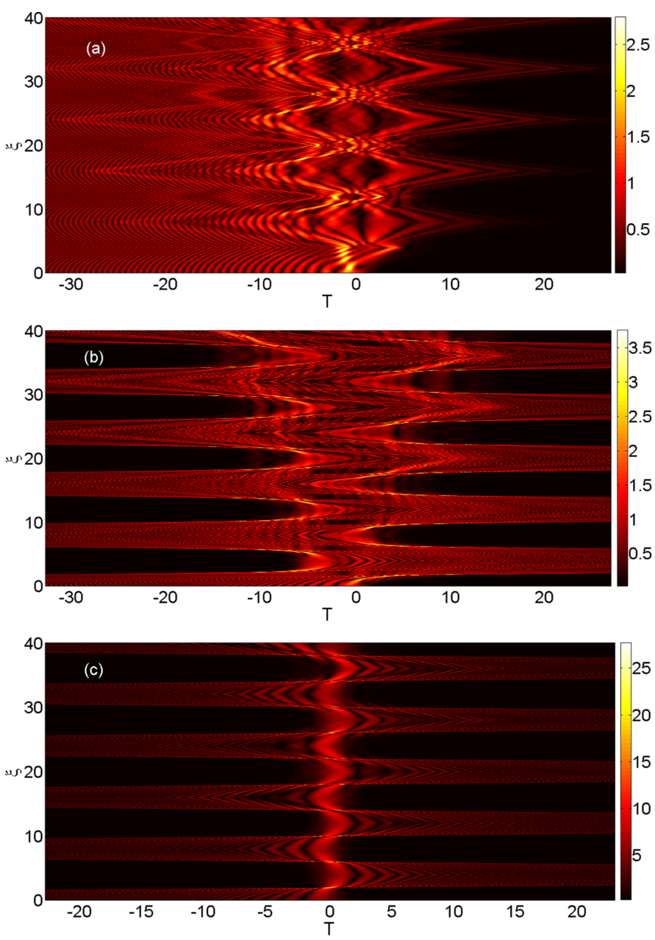

FIG. 2. (Color online) The dynamics of Airy pulses in the strongly nonlinear regime with the amplitude $A = 3$. The dynamics (a) for five periods of the DM scheme based on only SOD compensation and (b) for five periods of the DM scheme under equal action of SOD and TOD with $\epsilon = -1$. (c) Dynamics for 20 periods of the DM scheme under the dominance of TOD with $\epsilon = -1000$ and amplitude $A = 10$.

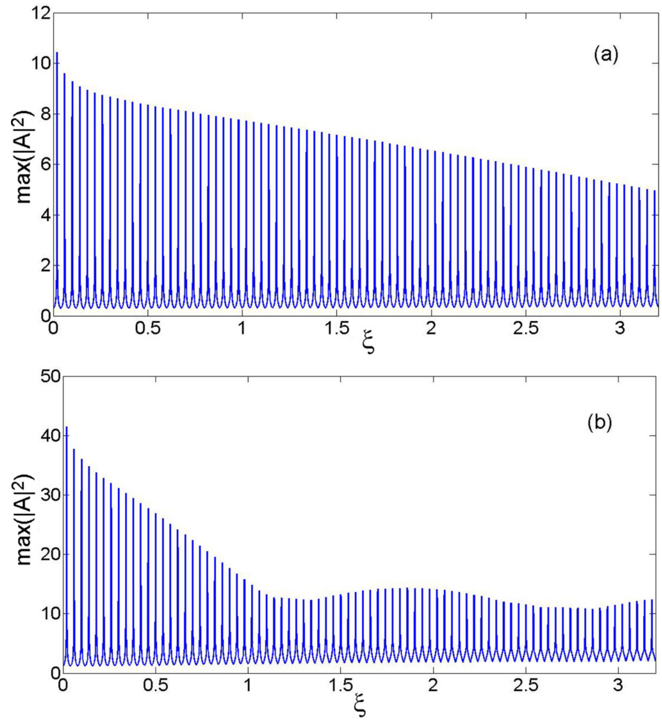

FIG. 3. (Color online) Evolution of the peak power of the Airy pulse in the strongly nonlinear regime for 40 periods of the DM scheme under the dominant action of TOD with $\epsilon = -100$ and an amplitude of (a) $A = 1$ and (b) $A = 2$.

One can reduce the negative effect of nonlinearity by choosing the central wavelength of the pulse to be near the zero-dispersion point of the fiber, which means working with a large ϵ. Figure 2(c) demonstrates such a dynamics in a highly nonlinear regime of an Airy pulse in a fiber link with $\epsilon = -1000$ as in Fig. 1(c) with an amplitude $A = 10$, which is 100 times higher than that pertaining to Fig. 1(c). It is shown that the pulse successfully propagates five DM periods with only some partial deformation.

For such a fiber link with pronounced dominance of TOD one can estimate the dependence of the system performance deterioration on the nonlinearity effect by studying the deterioration of the pulse's intensity enhancement with the distance for inputs with various amplitudes. This can be best observed at the focal points, where the pulse becomes mostly compressed. Figure 3 demonstrates the evolution of the peak intensity of an Airy pulse with amplitude $A = 1$ [Fig. 3(a)] and $A = 2$ [Fig. 3(b)] and with the truncation $\alpha = 0.001$ in a fiber link with 40 DM periods with $\epsilon = -100$. One can clearly see from Fig. 4 that 80 light hot spots are created within the propagation of the 40 DM periods. For the case of $A = 1$ presented in Fig. 3(a) the peak power ratio between its value at the focal points and at the input is partially reduced from 37.25 to 17.67 in the course of propagation of the 40 DM periods. In the case where nonlinearity has a stronger influence further degradation of the pulse compression and power enhancement at focal points is expected. Figure 3(b) reveals the much faster decrease in peak power enhancement for the input amplitude $A = 2$ within first 15 DM periods up to the propagated distance of about $\xi = 1.2$. Further the

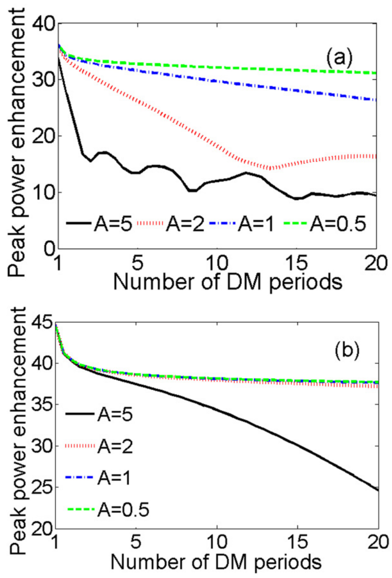

FIG. 4. (Color online) Reduction of the peak power enhancement in nonlinear propagation regimes with various pulse peak intensities for 20 periods of the DM scheme under the dominant action of TOD (a) with $\epsilon = -100$ and (b) with $\epsilon = -1000$. The green dashed, blue dot-dashed, red dotted, and black solid curves stand for the cases with $A = 0.5, 1, 2$, and 5, respectively.

decrease becomes less dramatic, showing oscillating behavior. Launching even more intensive pulses may also lead to solitons shedding out of the Airy pulse structure [20,28]. Figure 4(a) demonstrates the deterioration of the peak power enhancement with each of the 20 propagated DM periods with $\epsilon = -100$. The two cases of dynamics with injected amplitudes $A = 1,2$, corresponding to Fig. 3, are represented by the blue dot-dashed and red dotted curves, respectively. Additional cases of lower amplitude $A = 0.5$ (green dashed curve) and higher amplitude $A = 5$ (black solid curve) are also demonstrated.

One can achieve a significant improvement in the system performance working even closer to the zero-dispersion point of the fiber with the larger value of ε. Figure 4(b) demonstrates such an improvement for the same pulse dynamics as in Fig. 4(a), but with an increased value of the relative TOD strength parameter, $\epsilon = -1000$.

The cases with the injected amplitudes $A = 0.5, 1, 2$ almost overlap, demonstrating little degradation. The case with a very large amplitude $A = 5$ demonstrates a significant decrease in the pulse's peak power enhancement of about 45%, after the propagation of 20 DM periods, which is still much better than its counterpart in Fig. 4(a), which represents a 74% performance deterioration.

V. CONCLUSION

We have demonstrated a method for the regeneration of truncated self-accelerating Airy pulses in fiber links using the famous dispersion management technique in which fiber sections with opposite signs of the second- and third-order dispersion parameters are periodically alternating. In the low-power linear regime robust propagation of Airy pulses is limited only by fiber losses, and the dynamics of these pulses is fully described analytically. Comprehensive numerical studies demonstrate the qualitative validity of the main regeneration effect with good pulse shape maintenance also in the nonlinear regime. The system performance in the presence of a strong nonlinear effect can be further optimized by launching the input closer to the zero-dispersion point of fibers, which corresponds to increasing the relative strength of the third-order dispersion.

ACKNOWLEDGMENTS

The authors gratefully acknowledge support provided by the Deutsche Forschungsgemeinschaft (DFG) via the Research Training Group (GRK 1464) and computing time provided by PC2 (Paderborn Center for Parallel Computing).

[1] M. V. Berry and N. L. Balazs, Am. J. Phys. **47**, 264 (1979).
[2] G. A. Siviloglou, J. Broky, A. Dogariu, and D. N. Christodoulides, Phys. Rev. Lett. **99**, 213901 (2007).
[3] T. Ellenbogen, N. Voloch-Bloch, A. Ganany-Padowicz, and A. Arie, Nat. Photon. **3**, 395 (2009).
[4] I. Kaminer, M. Segev, and D. N. Christodoulides, Phys. Rev. Lett. **106**, 213903 (2011).
[5] N. K. Efremidis, Opt. Lett. **36**, 3006 (2011).
[6] Y. Hu, G. A. Siviloglou, P. Zhang, N. K. Efremidis, D. N. Christodoulides, and Z. Chen, in *Nonlinear Photonics and Novel Optical Phenomena* (Springer, New York, 2012), pp. 1–46.
[7] R. Driben, F. Mitschke, and N. Zhavoronkov, Opt. Express **18**, 25993 (2010); A. Demircan, Sh. Amiranashvili, and G. Steinmeyer, Phys. Rev. Lett. **106**, 163901 (2011); R. Driben and I. Babushkin, Opt. Lett. **37**, 5157 (2012); A. Demircan, Sh. Amiranashvili, C. Brée, C. Mahnke, F. Mitschke, and G. Steinmeyer, Appl. Phys. B (2013), doi: 10.1007/s00340-013-5609-9.
[8] G. A. Siviloglou and D. N. Christodoulides, Opt. Lett. **32**, 979 (2007).
[9] P. Saari, Opt. Express **16**, 10303 (2008).
[10] C. Ament, P. Polynkin, and J. V. Moloney, Phys. Rev. Lett. **107**, 243901 (2011).
[11] P. Piksarv, H. Valtna-Lukner, A. Valdmann, M. Lohmus, R. Matt, and P. Saari, Opt. Express **20**, 17220 (2012).
[12] Y. Hu, Z. Sun, D. Bongiovanni, D. Song, C. Lou, J. Xu, Z. Chen, and R. Morandotti, Opt. Lett. **37**, 3201 (2012).
[13] Y. Hu, M. Li, D. Bongiovanni, M. Clerici, J. Yao, Z. Chen, J. Azana, and R. Morandotti, Opt. Lett. **38**, 380 (2013).
[14] M. A. Preciado, Opt. Express **21**, 13394 (2013).
[15] A. Chong, W. H. Renninger, D. N. Christodoulides, and F. W. Wise, Nat. Photon. **4**, 103 (2010); D. Abdollahpour, S. Suntsov, D. G. Papazoglou, and S. Tzortzakis, Phys. Rev. Lett. **105**, 253901 (2010); W. P. Zhong, M. R. Belic, and T. Huang, Phys. Rev. A **88**, 033824 (2013).

[16] W. Liu, D. N. Neshev, I. V. Shadrivov, A. E. Miroshnichenko, and Y. S. Kivshar, Opt. Lett. **36**, 1164 (2011); P. Zhang, S. Wang, Y. Liu, X. Yin, C. Lu, Z. Chen, and X. Zhang, *ibid.* **36**, 3191 (2011); I. Epstein and A. Arie, Phys. Rev. Lett. **112**, 023903 (2014).
[17] J. Baumgartl, M. Mazilu, and K. Dholakia, Nat. Photon. **2**, 675 (2008).
[18] N. Voloch-Bloch, Y. Lereah, Y. Lilach, A. Gover, and A. Arie, Nature (London) **494**, 331 (2013).
[19] I. M. Besieris and A. M. Shaarawi, Phys. Rev. E **78**, 046605 (2008).
[20] R. Driben, Y. Hu, Z. Chen, B. A. Malomed, and R. Morandotti, Opt. Lett. **38**, 2499 (2013).
[21] W. Cai, L. Wang, and S. Wen, Optik **124**, 5833 (2013).
[22] I. Dolev, T. Ellenbogen, and A. Arie, Opt. Lett. **35**, 1581 (2010).
[23] N. J. Smith, F. M. Knox, N. J. Doran, K. J. Blow, and I. Bennion, Electron. Lett. **32**, 54 (1996); G. P. Agrawal, *Fiber-Optic Communications Systems*, 3rd ed. (Wiley, New York, 2002); R. Driben, B. A. Malomed, and P. Chu, Opt. Commun. **245**, 227 (2005); S. K. Turitsyn, B. G. Bale, and M. P. Fedoruk, Phys. Rep. **521**, 135 (2012).
[24] S. Wang, D. Fan, X. Bai, and X. Zeng, Phys. Rev. A **89**, 023802 (2014).
[25] G. P. Agrawal, *Nonlinear Fiber Optics*, 4th ed. (Springer, Berlin, Heidelberg, 2007).
[26] J. C. Travers, W. Chang, J. Nold, N. Y. Joly, and P. St. J. Russell, J. Opt. Soc. Am. B **28**, A11 (2011).
[27] S. K. Turitsyn, M. P. Fedoruk, and A. Gornakova, Opt. Lett. **24**, 869 (1999).
[28] Y. Fattal, A. Rudnick, and D. M. Marom, Opt. Express **19**, 17298 (2011); R. Driben, B. A. Malomed, A. V. Yulin, and D. V. Skryabin, Phys. Rev. A **87**, 063808 (2013); Y. Zhang, M. Belic, Z. Wu, H. Zheng, K. Lu, Y. Li, and Y. Zhang, Opt. Lett. **38**, 4585 (2013).